THE ROLE OF OCCLUDIN Ser471 IN ION PERMEABILITY

Aniket Ramshekar
University of Michigan
Senior Honors Thesis
8/14/2015

ABSTRACT

Tight junctions are dynamic cellular structures that are critical for compartmentalizing the apical and basal environments within tissues and regulating transport of small molecules, ions, and fluids. There are a plethora of protein families that comprise the tight junction (i.e. the three ZO families, over 24 claudin families, the MARVEL family, JAM family, etc) that are responsible for maintaining tight junction integrity. Studies have demonstrated that ZO-1, one of the tight junction proteins, is an organizer of tight junctions and claudins, another tight junction protein, contribute a critical role in establishing the barrier properties of the tight junction. However, recent studies have shown that occludin, a transmembrane protein, may also have regulatory functions in maintaining the tight junction. One of these functions is the phosphorylation-dependent binding of occludin to the protein ZO-1. Ser471, a phosphosite, is within a negatively charged region of the coiled-coil domain of occludin and interacts with ZO-1. Ongoing studies expressing phosphoinhibitory mutations of Ser471 (i.e. Ser471A) demonstrated that these mutants act in a dominant fashion to prevent proper tight junction formation and induce dramatic increase in solute permeability and ion flux. Previous studies have also demonstrated other mutants of occludin that may provide an ion specific alteration in permeability.

In this study, we tested the hypothesis that expression of Ser471A induces a non-selective ion flux due to observed gaps in tight junctions of Ser471A MDCK cells. To quantify the ion flux, experiments were performed using MDCK cell lines that expressed WTOcc, Ser471A, and Ser471D (n = 12) in an Ussing chamber and calculated, using the Goldman-Hodgkin-Katz and Kimizuka-Koketsu equations, the absolute permeability of sodium, potassium, and chloride ions.

We hypothesized that the malformed tight junctions in the Ser471A cell line will cause non-selective ion flux (i.e. an increase in absolute permeability for all three ions).

After measuring the permeability values for sodium, potassium, and chloride ions, we found that all three permeability values significantly increased in the Ser471A cell line compared to parental, WTOcc, and Ser471D ($P < 0.05$) suggesting non-specific ion flux. This study is consistent with ongoing research in the laboratory demonstrating that phosphorylation of Ser471 contributes to epithelial cell packing and proper tight junction formation.

Possible limitations of this project is that liquid junction potential was not taken into consideration and more cations and anions need to be tested. To further validate our findings, we will repeat the above protocol with the corrected equation to eliminate the liquid junction potential error and more ions to further justify the non-selective ion permeability in the Ser471A cell line.

Introduction:

Multicellular organisms require tissue barriers to help create and maintain defined environments. How these barriers are created and maintained remain an area of active research. Cells interact with one another through direct cell-cell junctions, or they may be bound together by extracellular materials that they secrete (Alberts et al., 2008). In either scenario, the formation of these interactions is imperative in order for cells to form tissues (i.e. epithelial, connective, muscle, nervous, and blood) and other larger structures (i.e. heart, brain, liver, lung, kidney, etc.).

There are two main ways animal cells are bound together: cell-cell adhesion and cell-matrix adhesion (Alberts et al., 2008). In connective tissue, the main stress-bearing component is the extracellular matrix and as a result the matrix bears mechanical stresses of tension and compression. In epithelial tissue, it is the cytoskeletons of the cells themselves, linked from cell to cell by anchoring junctions. The cell-matrix attachments bind epithelial tissue to the connective tissue below it and the cell-cell adhesion sites connect adjacent cells to one another. These cell adhesions are important because they can handle mechanical stresses, provide barriers between the extracellular and intracellular environment of an organism, organize directions of cell growth, and create blood tissue barriers.

Though binding cells to their environment is important (i.e. physical attachment) for both epithelia and in non-epithelial tissues, junctions between cell and cell or between cell and matrix are diverse in structure and have several other functions. There are four functional classes of cell junctions in animal tissues: anchoring junctions, channel-forming junctions, signal-relaying junctions, and tight junctions.

Anchoring Junctions:

There are four types of anchoring junctions: adherens junction, desmosome, actin-inked cell-matrix adhesion, and hemidesmosome. The former two are involved in cell-cell junctions and the latter two are involved in cell-matrix junctions. Transmembrane adhesion proteins play the central role for each of these anchoring junctions. These proteins span the membrane, with one end linked to the intracellular cytoskeleton and the other end linked to other extracellular structures. There are two superfamilies that these cytoskeleton-linked transmembrane fall into: cadherin and integrin. The former primarily mediates attachment of cell-to-cell, while the latter primarily mediates cell-to-matrix attachments. Each family is further classified based on their cellular connections (i.e. cadherins linked to actin form adherens junctions, while cadherins linked to intermediate filaments form desmosome junctions; integrins linked to actin form actin-linked cell-matrix adhesions, while integrins linked intermediate filaments form hemidesmosomes) (Alberts et al., 2008).

Adherens junctions connect actin filament bundles in one cell with that in the next cell. The transmembrane adhesion protein is known as E-cadherin for its presence in epithelial cells. These proteins make homophilic binding interactions with other cadherins on an adjacent cell. They bind with relatively low affinity, however, strong attachments result from the formation of many such weak bonds in parallel. The interaction among cadherins is analogous to that of a Velcro. Cadherins take their name from their dependence on Ca^{2+} ions. Studies have shown that adding Ca^{2+} ions to the extracellular medium causes adhesions mediated by cadherins to strengthen in mouse embryonic development (Alberts et al., 2008). These ions bind in the hinge regions in between adjacent cadherin domains. When Ca^{2+} is absent from the extracellular media,

the cadherins become flexible and the adhesion fails to form. In adherens junctions, cadherins are coupled indirectly to actin filaments via β-catenin, α-catenin, vinculin, and other anchor proteins. These junctions form a continuous adhesion belt near the apical surface of epithelial cells, encircling the interacting cells. The adhesion belt is tethered to actin filaments of the apical actomyosin belt. By indirectly linking actin filaments in one cell to those in its neighbors, adherens junctions coordinate the actomyosin-based forces among adjacent cells. The role of adherens junction interaction is to respond to increased cellular tension by strengthening their actin linkages. The importance of adherens junctions and their components is perhaps best understood by their role in human diseases. The cadherin–catenin complex directly contributes to cancer initiation and progression. Loss of E-cadherin and α-catenin in cancer cells results in loss of adhesion and promotes proliferation and invasion. Somatic mutations in E-cadherin in combination with a loss of heterozygosity are observed in a range of human carcinomas and occur early during tumorigenesis (Berx et al., 1998). A role for E-cadherin as a tumor suppressor is further suggested by the finding of germline mutations in diffuse gastric cancer and lobular breast cancer. Mutations in β-catenin have been observed in colon carcinoma, pilomatricoma and melanoma but these do not directly affect adherens junctions. Instead these mutations cause an increase in Wnt signaling, which directly affects the adherens junctions (Alberts et al., 2008).

Mutations in P-cadherin are found in hypotrichosis with juvenile macular dystrophy, a syndrome characterized by sparse and short hair and macular degeneration as well as a related ectodermal dysplasia syndrome called EEM (*e*ctodermal dysplasia, *e*ctrodactyly, *m*acular dystrophy). Interestingly, nectin-1 mutations are found in another ectodermal dysplasia syndrome associated with cleft lip and palate. The p120 members ARVCF and δ-catenin are mutated in a human syndrome associated with craniofacial with mental retardation and in Cri-du-

Chat syndrome associated with mental retardation, respectively. Overall, these mutations compromise the physiological function of adherens junctions (Lai-Cheong et al., 2007).

Desmosomes are another form of anchoring junction that connects intermediate filaments in one cell to those in the next cell. The transmembrane adhesion proteins are desmosomal cadherins (i.e. desmoglein and desmocolin). Desmosomes are structurally similar to adherens junctions, except the latter link to intermediate filaments instead of actin. The major function of desmosomes is to provide mechanical strength. To form this junction, plakoglobin and plakophilin bind to cytoplasmic tail of desmoglein and desmocolin and bind to desmoplakin, which in turn binds to intermediate filaments. When adjacent cells are indirectly connected to one another through this intermediate filament network, the junction is known as a desmosome. Disruption of the desmosomes can result in the detachment of the epithelial from the basal layer. An example of such a clinical manifestation is epidermis bullosa, which is skin blistering resulting from mutant keratin genes (i.e. disrupted desmosome) that leads to rupturing of cells in the basal layer of the epidermis (Alberts et al., 2008).

On the other hand, if the intermediate filament network is attached to the cell on one side and the basal lamina on the other, the junction is called hemidesmosomes. An example of a clinical disorder involving hemidesmosomes is bullous pemphigoid. This disorder is an acute or chronic autoimmune skin disease, involving the formation of blisters at the space between the skin layers of epidermis and dermis caused by the body forming anti-hemidesmosome antibodies (Wolff et al., 2007). This autoimmune disorder is acquired mainly through exposure to ultraviolet light and radiation therapy (Chan, 2011).

Channel-Forming Junctions:

Gap junctions or channel-forming junctions are present in most animal tissues, including connective tissues as well as epithelia, allowing the cells to communicate with other adjacent cells. This junction allows the cytoplasmic content of one cell to form a direct passageway to the cytoplasmic content of another cell. The combinations of connexins that comprise gap junctions determine the properties of the junctions. Connexins are four-pass transmembrane proteins, six of which assemble to form a hemichannel, or a connexon. When the connexons in the plasma membranes of two cells come in contact and are aligned, they form a continuous aqueous channel that connect the two cell interiors (Alberts et al., 2008). These intercellular channels can be homotypic or heterotypic depending on the type of connexons that come together. Functions of these channels are diverse. A classic example is the gap junctions present in the heart to cause synchronous muscle contraction to maintain a heartbeat. Also, the cell can dynamically control these gap junctions. For instance, cytosolic pH changes can cause the channel to open or close to maintain physiological conditions by changing the permeability of various ions (Alberts et al., 2008). In addition, gap junctions relay cell death signals from one apoptotic cell to the neighboring cell. This can cause otherwise unaffected, healthy adjacent cells to also go through apoptosis. This phenomenon is known as the bystander effect because of its ability of killing bystander cells regardless of their condition (Li Bi et al., 1993).

Signal-Relaying Junctions:

Anchoring, occluding, and channel-forming junctions all are capable of having signaling functions in addition to their structural roles. Examples of signal-relaying junctions include chemical synapses in the nervous system and immunological synapses in the immune system. Also the classic transmembrane ligand-receptor cell-cell signaling contacts (e.g. Delta-Notch, ephrin-Eph, etc.) are another form of signal-relaying junction (Alberts et al., 2008). An example of signal-relaying junction is the chemical synapse in the nervous system. In this junction an electrical impulse from neurons triggers the release of neurotransmitters in the synaptic cleft. Disruption of this system can lead to various disorders (i.e. myasthenia gravis and Lambert-Eaton myasthenic syndrome).

Tight Junctions:

The epithelial cells are attached to one side known as the basal side and free of any anchorage on their opposite side – the apical side (Farquhar and Palade, 1963; Claude and Goodenough, 1973). One function of all epithelia is to serve as a selective, permeable barrier - separating the fluid on the apical and basal side from mixing with one another. There are more specialized functions of epithelia depending on their location in the body. For example, kidney epithelia allow filtration of blood and reuptake of essential blood borne material. In order to fulfill this function, adjacent kidney epithelial cells are sealed together by occluding junctions to prevent apical content from mixing with that of the basal.

Likewise, occluding junctions in vertebral, epithelial small intestine cells fulfill a similar role. The small intestine is comprised of simple columnar epithelia (Alberts et al., 2008) that are responsible for the uptake of nutrients from the lumen of the gut and transport of these nutrients to the blood vessel. There are channels and proteins that are directed to the apical side of the epithelium and proteins directed to the basal side. The localization of proteins is imperative to maintain function of the small intestine. For example, the sodium-driven glucose symporter must be directed to the apical side so that glucose can diffuse from one side of the gradient to the other. Therefore, some structure in the cell must play an important role in maintaining proper localization of these channel proteins to their correct positions (i.e. apical or basal). It has been shown that tight junctions between epithelial cells may function to help separate domains within the plasma membrane to prevent drifting of the protein to the wrong side of the membrane (Alberts et al., 2008). In addition, tight junctions also facilitate the maintenance of a concentration gradient (i.e. prevent apical content from mixing with the basal content) by occluding adjacent epithelial cells in the most apical position. Through this function, tight junctions ensure the active transport of glucose from the lumen of the gut to the blood to nourish our body (i.e. transcellular transport) by preventing the apical content and basal content from mixing as well as directing channel proteins to their appropriate location in the cell.

In order to function, tight junctions are comprised of multiple proteins known as tight junction proteins. The first tight junction protein identified was the scaffolding protein known as the zonula occludens (i.e. ZO proteins) (Stevenson et al., 1986). There are three classes of ZO: ZO-1, ZO-2, and ZO-3. The scaffolding proteins ZO-1, ZO-2, and ZO-3 play a unique role in the organization and regulation of tight junctions. These proteins are members of a family of membrane associated signaling proteins known as the membrane-associated guanylate kinase

homologs (MAGUKs) (Woods et al, 1993). Members of this family are distinguished by a core cassette of protein-binding domains, which include one or more PSD95/ dlg/ZO-1 (PDZ) domains, an SH3 domain, and a region of homology to guanylate kinase (GuK) (Fanning et al., 1998). The function of the ZO proteins is to mediate binding to transmembrane tight junction proteins (Beatch et al., 1996; Stevenson et al., 1986) to form the diffusion barrier to separate the cell to apical and basolateral compartments (Umeda et al., 2006).

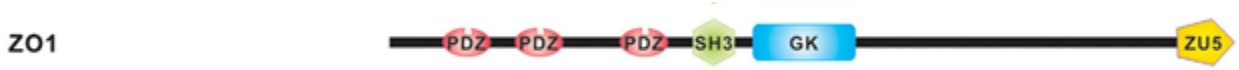

Figure 1. Domain Organization of the ZO-1 protein. These proteins are sub-families of MAGUK scaffolds and are known to function as structural organizer of the tight junction (Zhu et al., 2011).

In a freeze fracture electron microscopy, the tight junctions appear as a network of sealing strands that encircle each cell on the apical side in the epithelial sheet (Staehelin, 1974). In conventional electron microscopy, the two plasma membranes interacting appear to be tightly apposed where sealing strands are present. In addition to these observational conclusions from microscopy, it was identified that each tight junction sealing-strand is made up of a long row of transmembrane adhesion proteins (Alberts et al., 2008) besides the ZO proteins.

One of these proteins in the tight junction sealing strand is occludin, which is a tetrapass transmembrane protein that is ~65 kDa (Schneeberger and Lynch, 2004). Occludin – from the Latin word meaning ‘to block’ – was named because, at the time of its discovery, it was the only protein discovered in the most apical cellular region and was thought to play the main role in occluding paracellular flux (Furuse et al., 1993). Occludin has a long COOH-terminal cytoplasmic domain, a short NH2-terminal cytoplasmic domain, two extracellular loops, and one

intracellular turn. One of the most distinguishing features of its sequence is the high content of tyrosine and glycine residues in the first extracellular loop (~60%) (Saitou et al., 2000).

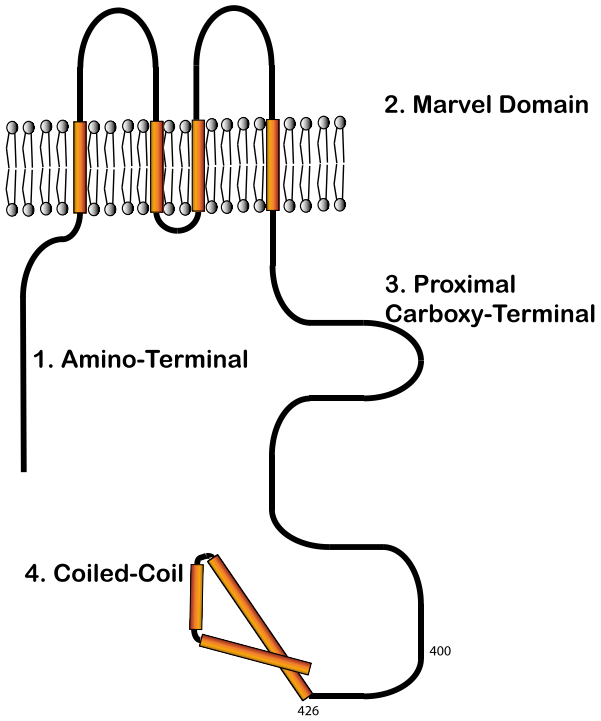

Figure 2. Diagram of Occludin Domains. Occludin is a tetraspan protein. The first extracellular loop of occludin is rich in tyrosine and glycine residues, and neither loop has a significant number of charged amino acid residues (image courtesy of Dr. David A. Antonetti).

The function of occludin was partially identified by occluding gene deletion in in mice (Saitu et al., 2000). Through this molecular technique, the phenotype of the mice altered considerably when compared to wild type mice. For example, all occludin knockout mice had

postnatal growth retardation, the occludin knockout male mice produced no offspring when mated with either wild type or occludin knockdown females, the occludin knockout females did not exhibit proper weaning behavior after giving birth, and thinning of the compact bone in both genders were observed (Saitou et al., 2000). One explanation of this result is that tight junctions exist in gastrointestinal epithelium and lack of occludin may affect Ca^{2+} uptake through the paracellular pathway. Likewise in mice, there are tight junctions in the Sertoli cells that may cause improper spermatogenesis causing sterility (Saitou et al., 2000). Even though multiple pathological events were noted in these knock out mice, the tight junction barrier did not change electrophysiologically. This outcome suggested that occludin is not the protein responsible for occluding paracellular flux, contrary to its name, and that another protein is responsible for this occlusion (Furuse et al., 1998). However, the multiple phenotypical changes suggested important roles in tissues regarding tight junctions. For example, the use of siRNA directed to occludin resulted in a selective increase in paracellular permeability of small organic cations (Yu et al., 2005).

However prior to that study, further validation that occludin was not the protein responsible for barrier formation was obtained when a mutated occludin, one that was COOH-terminally truncated, was stably transfected into MDCK cells. This mutation did not affect the continuous network of tight junction strands (Balda et al., 1996). It was also shown that disruption of occludin genes in embryonic stem cells still led to the differentiation into epithelial cells with well-developed tight junctions (Furuse et al., 1998). These data confirm that there exists another protein that is also responsible for maintaining the tight junction integrity in addition to occludin and ZO. Claudins – named for the Latin word ‘claudere’ meaning to close – is the most essential protein for tight junction formation and function (Umeda et al., 2006).

Claudins are tetrapass transmembrane proteins that have no sequence homology to occludins (Furuse et al., 1998). There are twenty-four claudin family members differentially expressed in different tissues and the amino acid composition of the two extracellular loops of claudins varies considerably, which affects ion and/or size selectivity of tight junction (Alberts et al., 2008).

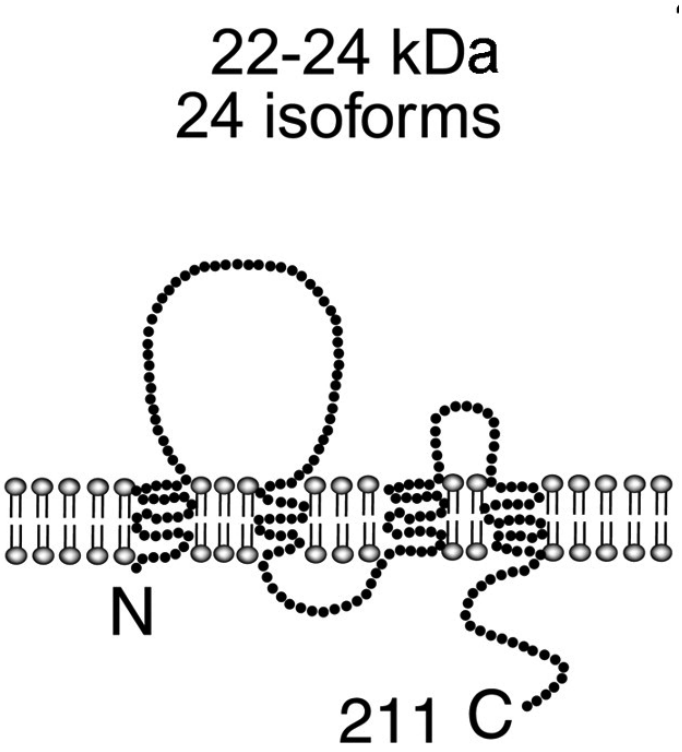

Figure 3. Diagram of Claudin-1. The amino acid composition of the two extracellular loops of claudin varies significantly among other claudins, resulting in a wide range of isoelectric points (Schneeberger and Lynch, 2004).

It has been shown, using recombination methods, that there are portions of the ZO-1 and ZO-2 scaffolding proteins that allow for the independent determination of whether and where claudins are polymerized in the tight junction (Umeda et al., 2006). This relationship suggests that the tight junction is actually a complex of various proteins that are interacting with one another to form the barrier between the apical side and basal side of the epithelium. Another interaction in the tight junction sealing-strands are between rows of claudin and occludin transmembrane adhesion proteins embedded in the plasma membrane of two interacting cells. It has been hypothesized that the extracellular domains of claudin and occludin bind the proteins to one another and the intracellular termini interact with the scaffolding proteins that link the tight junction to actin (Alberts et al., 2008).

These interactions among tight junction proteins (i.e. claudin, occludin, ZO) can dynamically change in response to various extracellular stimuli (Shen et al., 2008). It has been demonstrated through fluorescence recovery after photobleaching and other methods that the majority of occludin diffuses rapidly within the tight junction. In contrast, the majority of claudin-1 is stabilized at the tight junction complex when compared to occludin, however, claudin-1 still is localized under different environmental conditions (Shen et al., 2008). Overall, the majority of tight junction associated ZO-1, occludin, claudin-1, and β-actin do not remain bound in a complex at steady state. This suggests that at various environmental conditions, the epithelial cells are able to adapt to their surroundings by changing the integrity of their tight junction to modify permeability and that mutational analysis of claudins reveal proteins in this family regulate ion flux.

However, even though occludin is not required for basal barrier (i.e. ion flux) properties of epithelia as suggested by occludin knockout mice, phosphorylation of occludin has been

shown to play an important role in regulating barrier properties. For instance, changes in occludin phosphorylation states have been associated with increased endothelial permeability in response to vascular endothelial growth factor (Antonetti et al., 1999; Harhaj et al., 2006). There are also several other studies relating the site-specific occludin phosphorylation to occludin function.

For example, T403 and T404 occludin phosphorylation enhance both the trafficking of the protein to the tight junction and paracellular barrier function (Suzuki et al., 2009). Whereas, phosphorylation of occludin sites Y398 and Y402 reduces occludin–ZO-1 interactions, interferes with occludin localization at the tight junction, and sensitizes monolayers to oxidant-induced barrier disruption (Elias et al., 2009). Similarly, phosphorylation of the more distal occludin S490 site, which is located within the C-terminal coiled-coil occludin/ELL OCEL domain, attenuates the interaction between occludin and ZO-1 (Sundstrom et al., 2009) and is associated with occludin endocytosis and barrier loss in endothelial cells in response to vascular endothelial growth factor (Murakami et al., 2009). Another site on occludin that is phosphorylated is Ser408. CK2-mediated phosphorylation of occludin S408 controls the interactions between occludin, ZO-1, claudin-1, and claudin-2, and suggest S408 phosphorylation as a molecular switch that regulates tight junction structure and paracellular pore pathway flux. (Raleigh et al., 2011).

There has also been evidence that mutations in Ser471 on occludin can cause changes in the regulation of tight junction barrier properties. It has been shown that this specific site may enhance occludin:ZO-1 complex stability (Tash et al., 2012). To test this hypothesis, the serine residue at site 471 was replaced with aspartic acid (i.e. Ser471D) – a phosphomimetic mutation. The point mutated occludin was then transiently transfected into MDCK cells and upon observation using a confocal microscopy, the mutated occludin demonstrated good apical border

co-localization with ZO-1 (Tash et al., 2012). Also it was shown by using peptides with and without a phosphogroup on Ser471 that the capture of the PDZ3-SH3-GuK (PSG) domain, the point of interaction between occludin and ZO, of ZO-1 is inhibited more by the phosphogroup peptide than the peptide without a phosphogroup (Tash et al., 2012). These results suggest that the acidic head of the occludin coiled coil domain interacts with the GuK domain of PSG with high affinity and phosphorylation of Ser471 enhances occludin:ZO-1 complex stability (Tash et al., 2012). Collectively, these studies reveal that occludin acts in a phospho-dependent manner to regulate cellular processes associated with the tight junction complex. However, the role of Ser471 phosphorylation was incompletely understood. The location of this site within a ZO-1 contact point suggested a potential role in tight junction and cellular function.

Current Studies:

To determine the role of Ser471 phosphorylation, stable cell lines expressing point mutants were created. Madine Darby Canine Kidney (MDCK) cells were selected as these readily form tight junctions and have been well-characterized in junctional properties. The cell lines created included; wild-type occludin (WTOcc) and in order to determine if phosphorylation of Ser471 contributes to barrier function, a phosphoinhibitory mutation was made by changing the wild type serine at occludin site 471 to alanine (i.e. Ser471A). Serine was changed to alanine because the latter amino acid lacks a hydroxyl group making the mutated occludin incapable of being phosphorylated at this site (Figure 4). This is known as a phosphoinhibitory mutation because the alanine does not bear a hydroxyl group on its side chain and therefore cannot be phosphorylated by kinases. In addition, a phosphomimetic mutation was made by replacing

serine at site 471 with a negatively charged aspartic acid (i.e. Ser471D). It was hypothesized that the state of phosphorylation at 471 would affect tight junction integrity and as a result change the transepithelial resistance and permeability of ions and solutes.

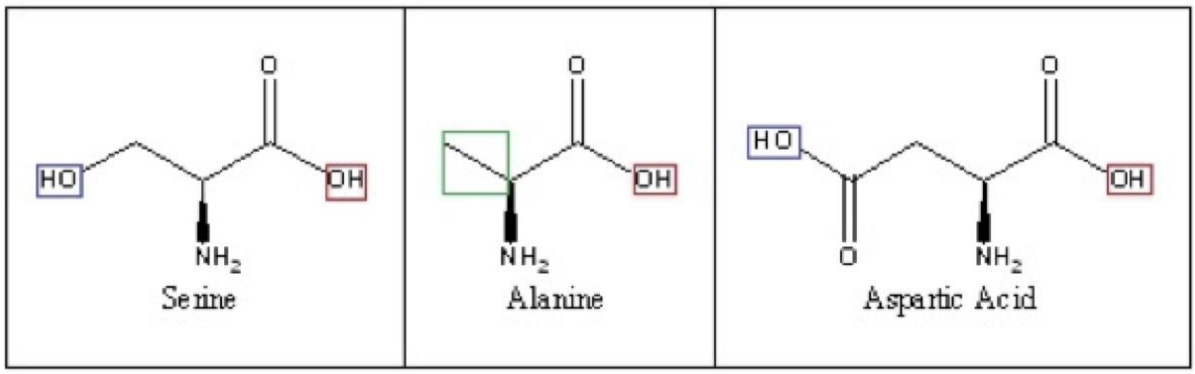

Figure 4. Structure of the Amino Acids. Serine is the amino acid that is present in the WTOcc 471 site. There are structural similarities between alanine and serine. The main difference is the presence of a methyl group (green) on alanine and lack of a phosphorylation site (i.e. phosphoinhibitory). Aspartic acid has a carboxyl group (blue) making the amino acid bear an overall negative charge just as a phosphate group making it a phosphomimetic. The hydroxyl groups in red do not perform in phosphorylation because they are involved in forming peptide bonds.

The studies reveal that overexpressing Ser471AOcc significantly reduces transepithelial resistance when compared with WTOcc, whereas there was no significant drop in transepithelial resistance for the Ser471D line (Figure 6 and 7). Further, the barrier to TAMRA, a ~400 Da fluorescent molecule, was also dramatically reduced in the Ser471A expressing cells compared to WTOcc while Ser471D did not demonstrate any change (data not shown). In addition, immunocytochemistry reveal large breaks in tight junction strands in the Ser471A expressing

cell lines compared to WTOcc or Ser471D expressing cells (Figure 5). These data suggest that the phosphosite at Ser471 may play a role in regulating formation or maintenance of tight junctions.

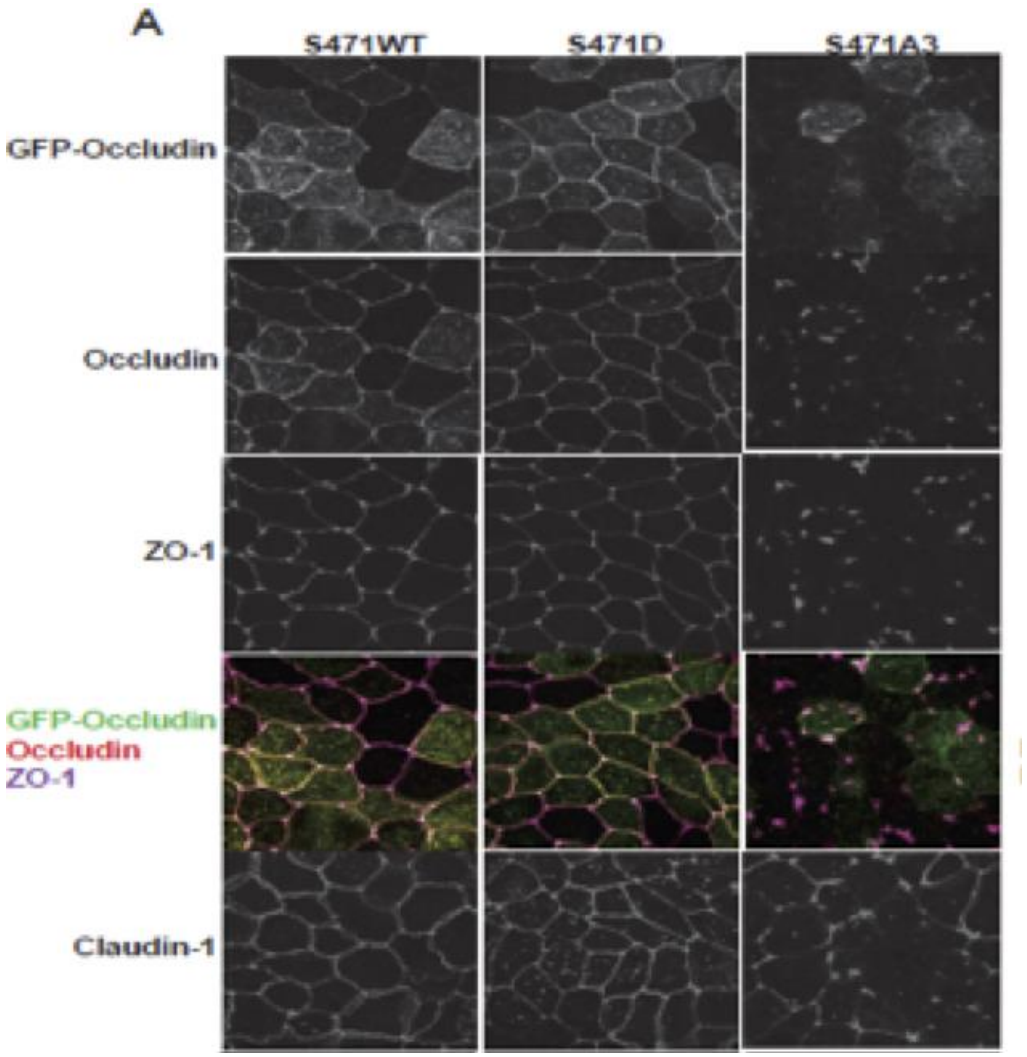

Figure 5. Tight Junction Proteins are Mislocalized in Occludin Ser471A Mutant Cell Lines. Immunocytochemical maximum projected stacks (3 μm thick) of indicated proteins using a 63x confocal objective with 5x zoom for tight junction proteins (image courtesy of Mark Bolinger).

Changes in electrical resistance could be due to small pores forming specific ion channels as observed for Ser408 phosphorylation of occludin (Turner et al., 2012) or may be due to large gaps in the junction complex leading to non-specific ion flux. The observed alterations in tight junction immunofluorescence microscopy suggested the latter but quantitative data of specific ion flux would provide critical data to support this model. The project was designed to identify if the decrease in transepithelial resistance in the Ser471A line was due to changes in specific ion flux or a generalized change in ion flux. Therefore, an electrophysiological study of the MDCK occludin mutant cell lines was conducted. To set up this experiment, an Ussing chamber apparatus was utilized. This apparatus allows rapid control of the basal and apical environmental conditions by introducing various solutions. In this study, Ringer solution was initially used (Table 1) on both the apical and basal sides. Transepithelial resistance was measured by inducing a bipolar current of 20 μA. The diffusion transepithelial potential was measured by changing the solution on either the apical or basal side. By using the Goldman-Hodgkin-Katz and Kimizuka-Koketsu equations, we were able to calculate the absolute permeability of the ions (i.e. sodium, potassium, and chloride). We hypothesize that since the Ser471A cell line had the lowest transepithelial resistance and improper tight junction formation, the Ser471A should have the highest permeability for all the ions being tested – implying nonspecific ion flux.

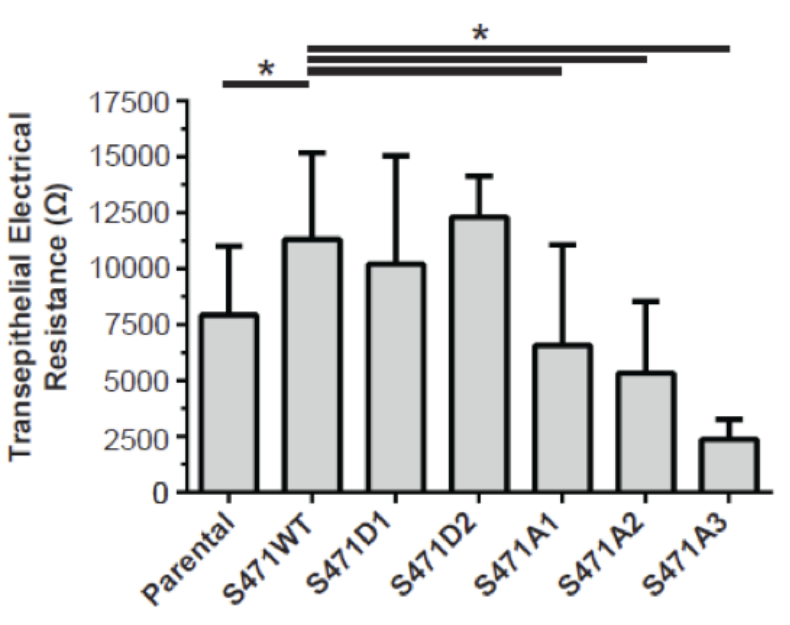

Figure 6. Phosphoinhibitory (Ser471A) Lines are "Leaky" Compared to Ser471D or WT. Trans-epithelial electrical resistance 3 days post confluent (image courtesy of Mark Bolinger).

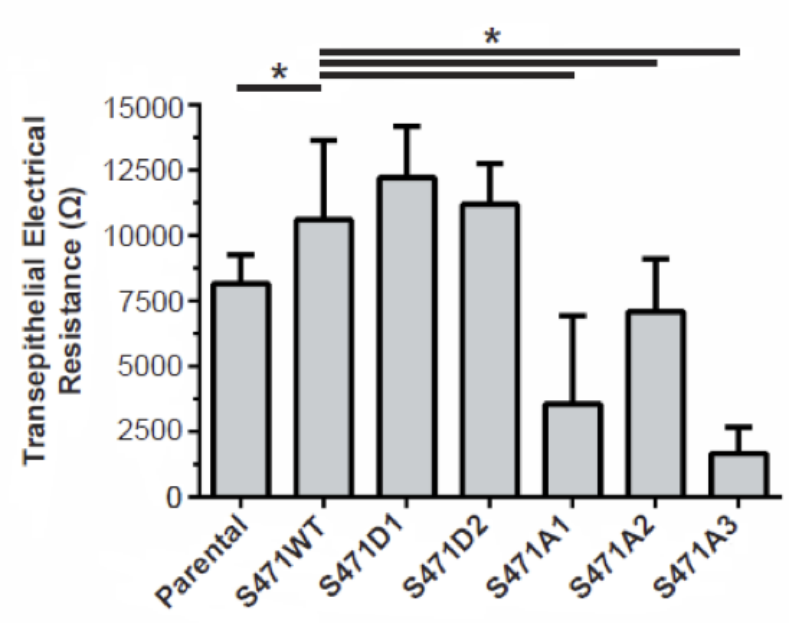

Figure 7. Phosphoinhibitory (Ser471A) Lines are "Leaky" Compared to Ser471D or WTOcc. Trans-epithelial electrical resistance 4 days post confluent (image courtesy of Mark Bolinger).

Materials and Methods:

MDCK cells:

Madine-Darby Canine Kidney (MDCK) cells were originally derived from the kidneys of a normal male cocker spaniel in 1958 (Cho et al., 1989). When these cells are grown on a porous membrane, they form a confluent monolayer with well-developed intercellular occludin junctions (Misfeldt et al., 1976; Cereijido et al., 1978). The original MDCK cells used in our experiments were obtained from ATTC. To transfect the plasmids with a plasmid (Figure 8) the Lipofectamine 2000 protocol was used.

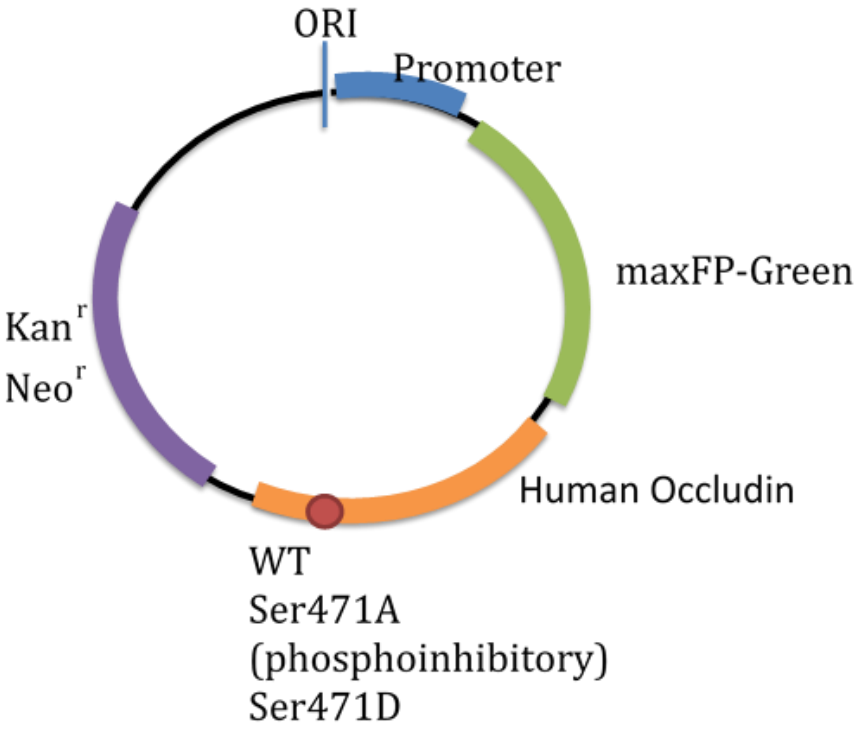

Figure 8. Fusion-protein construct transfected into MDCK cells. The red dot represents the approximate site at which the mutation is made.

To plate the MDCK cells/lines on the transwell, they were first trypsinized for 15 minutes and then counted on a hemocytometer. 130,000 cells were plated in each well with 300 μL MEM MDCK cell media and 500 μL media placed outside the transwell. Cells were then monitored via microscope daily. Confluence typically occurred around two days after plating, at which point experiments were carried out on the fourth day post confluence because it was noted through experience that this is the optimal time it took the MDCK cells to form a tight monolayer. The media was changed daily between plating and the experiment to facilitate the health of the cell.

Millicell:

All MDCK cells were cultured on Millicell-CM Biopore (EMD Millipore, Billerica, MA) membranes (hydrophilic PTFE cell culture insert with pore size of 0.4 μm used in a 24-well plate).

Ringer Solutions:

Hepes ringer solutions are buffered solutions made to mimic physiological conditions in the cell. The ringer solution that contains the full concentration composition will be abbreviated as HR, whereas the ringer solution with the concentration of the ion reduced will be referred to as XHR, where X will equal to the percent of the ion present from the original. For example when the sodium concentration was diluted by 75% compared to the original HR, the reference to this solution is $0.25[Na^+]HR$.

The concentration of sodium was dropped by 75% so that a comparable difference between the HR on the apical on basal side versus inducing a concentration gradient when measuring voltage potential via the Ussing chamber. In order to balance the osmolarity of the solution when reducing the concentration of sodium in ringer solution, we added the appropriate amount of mannitol. This same procedure was followed in making the ringer solution for potassium ion. The ingredients for the solutions used (i.e. HR, 0.25[Na^+]HR, and 0.25[K^+]HR) is detailed in Tables 1, 2, and 3, respectively.

HR	
Chemical	**mM**
NaCl	135
KCl	5
HEPES	10
Glucose	10
$CaCl_2$	1.8
$MgCl_2$	1

Table 1. Ingredients of a Hepes Ringer (HR) Solution. The appropriate amount of mannitol was used to balance the osmolarity of the solution.

0.25[K+]HR	
Chemical	**mM**
NaCl	135
KCl	1.25
HEPES	10
Glucose	10
$CaCl_2$	1.8
$MgCl_2$	1

Table 2. Ingredients of a Hepes Ringer Solution with Diluted [K^+]. The appropriate amount of mannitol was used to balance the osmolarity of the solution.

0.25[Na+]HR	
Chemical	**mM**
NaCl	33.75
Mannitol	101.25
KCl	5
HEPES	10
Glucose	10
$CaCl_2$	1.8
$MgCl_2$	1

Table 3. Ingredients of a Hepes Ringer Solution with Diluted [Na^+]. The appropriate amount of mannitol was used to balance the osmolarity of the solution.

Electrophysiology Methods and Calculations:

Electrophysiological recordings were performed on epithelial monolayers in an Ussing chamber (Harvard Apparatus #U9926/T) (Figure 9). Voltage and current clamps were performed using the EC-800 epithelial amplifier (Warner Instruments) with Ag/AgCl electrodes and an Agarose bridge containing 3M KCl. The transepithelial resistance was measured under the 'Resistance' mode by passing a constant bipolar current pulse (I_o) of 20 µA through the epithelium and recording voltage deflection (V_o). Ohm's law was used to calculate transepithelial resistance from Vo and Io. The series resistance was measured in absence of the epithelium and subtracted from the transpithelial resistance. Dilution potentials were measured under the 'Current Clamp' mode by clamping the transepithelial current to zero and recording the equilibrium voltage generated by NaCl diffusion. All experiments were conducted at 37º C. Electrical potentials obtained from blank inserts were subtracted from those obtained from inserts with epithelial monolayers as published in other literature (Hou et al., 2005). Transepithelial resistance of the confluent monolayer of cells was determined in Ringer solution (135 mM NaCl, 5 mM KCl, 10 mM HEPES, 10 mM glucose, 1.8 mM $CaCl_2$, 1 mM $MgCl_2$). Dilution potentials were measured when buffer B (33.75 mM NaCl, 5 mM KCl, 10 mM HEPES, 10 mM glucose, 1.8 mM $CaCl_2$, 1 mM $MgCl_2$) or buffer C (135 mM NaCl, 1.25 mM KCl, 10 mM HEPES, 10 mM glucose, 1.8 mM $CaCl_2$, 1 mM $MgCl_2$) replaced Ringer solution on the apical side or basal side of the epithelium.

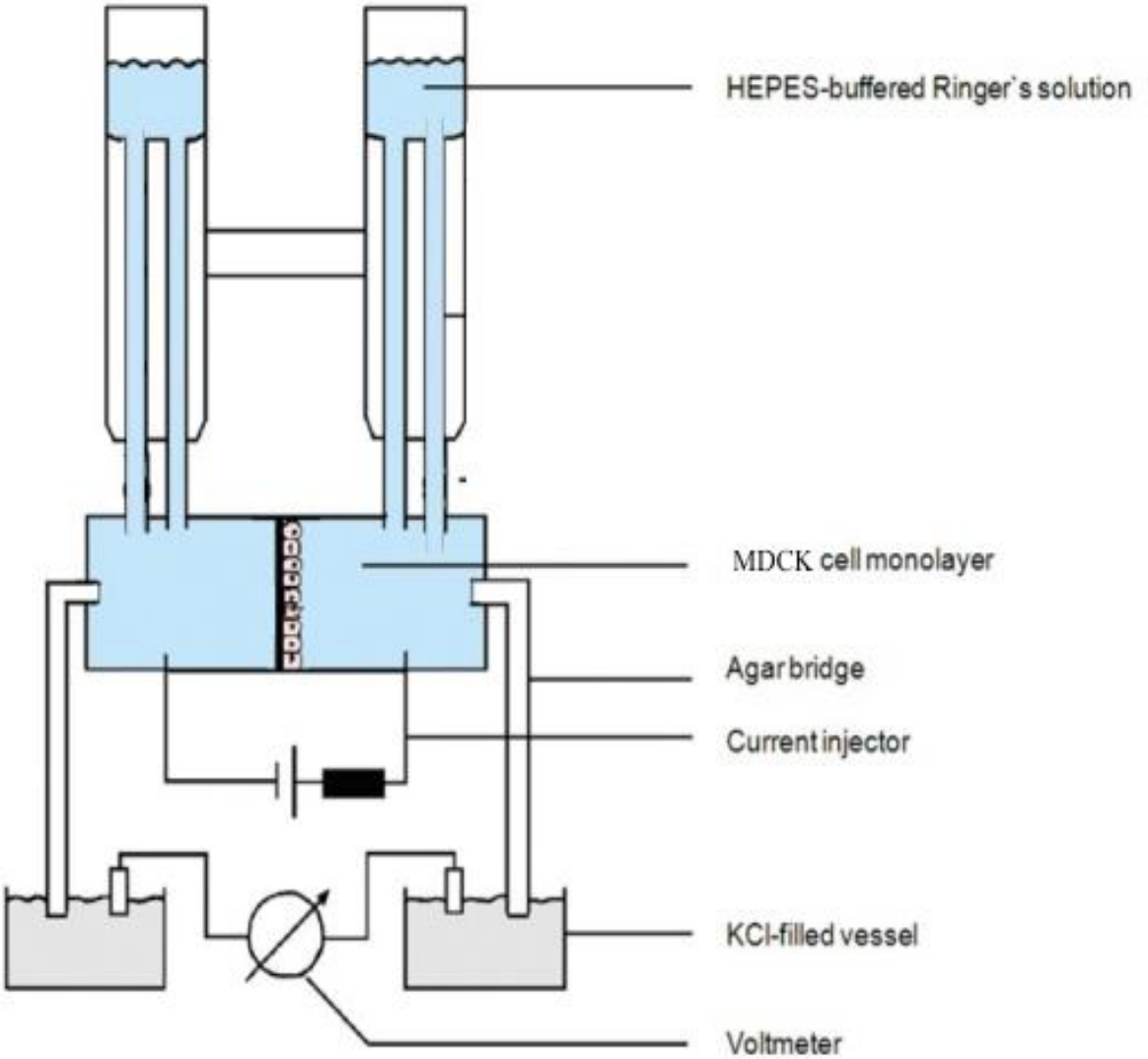

Figure 9. Diagram Detailing the Various Components of an Ussing chamber. In order to find out the permeability ratio the solution in either the apical side or basal side was changed to a different concentration of sodium. The reference was the basal side of the membrane (modified after Li et al., 2004).

The ion permeability ratio for the monolayer was calculated from the dilution potential using the Goldman-Hodgkin-Katz equation:

$$\eta = -(\varepsilon - e^{v}) / (1 - \varepsilon e^{v}),$$

where η is the ratio of permeability of the monolayer to Na^+ over the permeability of to Cl^- ($\eta = P_{Na}/P_{Cl}$); ε is the dilution factor ($\varepsilon = C_{basal}/C_{apical}$); $v = eV/kT$ (V is the dilution potential, k is the Boltzmann constant, e is the elementary charge and T is the temperature in Kelvins). The condition we use this equation is only when we induce a concentration gradient by filling the apical and basal sides of the Ussing chamber with unsymmetrical solutions. Using the permeability ratio derived from using the Goldman-Hodgkin-Katz equation, the absolute permeabilities of sodium and chloride were calculated by using the simplified Kimizuka-Koketsu equation:

$$P_{Na} = (G / C) * (RT / F^2) * (\eta / (1 + \eta))$$
$$P_{Cl} = (G / C) * (RT / F^2) * (1 / (1 + \eta)),$$

Where G is the total conductance of the membrane that can be measured by Ohm's law ($V = I*R$ or $G = I/V$), C is the concentration of ion in solution, R is the gas constant, F is the Faraday constant, and η is the ratio of permeability of the monolayer to Na^+ over the permeability of to Cl^-. The permeability of K^+ was measured similarly to Na^+ (with the chemical gradient of 5 mM to 1.25 mM). The dimensional analysis is provided below to assist in calculations:

$$\nu = \frac{eV}{kT} = \frac{C * \frac{kg*m^2}{s^3*A}}{\frac{m^2*kg}{s^2*K} * K} = \frac{A * s * \frac{kg*m^2}{s^3*A}}{\frac{m^2*kg}{s^2*K} * K} = 1$$

$$\eta = \frac{-(\varepsilon - e^{\nu})}{(1 - \varepsilon e^{\nu})} = 1$$

$$P_{Na} = \frac{G}{C} * \frac{R*T}{F^2} * \frac{\eta}{1+\eta} = \frac{\frac{1}{\Omega*m^2}}{M} * \frac{\frac{V*C}{K*mol} * K}{\frac{C}{mol} * \frac{C}{mol}} * \frac{\eta}{1+\eta} = \frac{\frac{A}{V*m^2}}{\frac{mol}{L}} * \frac{V}{\frac{C}{mol}} * \frac{\eta}{1+\eta}$$

$$= \frac{A*L}{m^2} * \frac{1}{C} * \frac{\eta}{1+\eta} = \frac{\frac{C}{S}*L}{m^2} * \frac{1}{C} * \frac{\eta}{1+\eta} = \frac{\frac{C}{S}*m^3}{m^2} * \frac{1}{C} * \frac{\eta}{1+\eta} = \frac{m}{s}$$

Statistical Analysis:

A one-way ANOVA with Bonferroni post-hoc test was used to determine whether or not there is a statistical difference in the permeability of sodium ions in the different Ser471 occludin mutants of MDCK. Normalization of each cell line to WTOcc was made because WTOcc had the overexpressed human occludin and so do Ser471A and Ser471D. By normalizing using WTOcc values, it will eliminate overexpression of human occludin as an extraneous factor. Values are expressed as the mean ± standard deviation unless otherwise stated.

Results:

Transepithelial resistance:

MDCK cells were grown to confluence on membrane filters and inserted into the Ussing chamber. Hepes ringer solution was applied to both sides and Ohm's Law was used to calculate transepithelial resistance after application of bipolar current. The transepithelial resistance for the occludin Ser471A mutant cell line (28.9 ± 3.7 $\Omega*cm^2$) was significantly lower compared to that of the WTOcc (45 ± 15.8 $\Omega*cm^2$), Ser471D (44 ± 6.8 $\Omega*cm^2$), and parental cell lines (51 ± 13 $\Omega*cm^2$) ($P < 0.05$) (Figure 10, Table 4). The transepithelial resistance of the Ser471D, however, was approximately the same as that of the WTOcc and parental. These relative values are consistent with earlier recordings using the ECIS real-time measurement of electrical resistance in which the Ser471A line had a lower recorded transepithelial resistance compared to that of the WTOcc (Figures 6, 7).

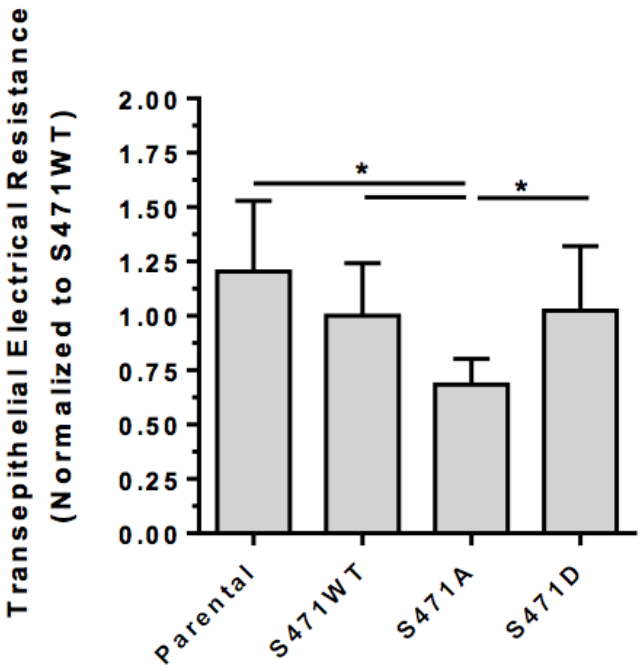

Figure 10. Normalized Transepithelial Resistance for Each of the Cell Lines. Data expressed as Mean ± SD (n = 12). *P < 0.05 compared to parental, Ser471WT, and Ser471D.

Group	Parental	WTOcc	Ser471A	Ser471D
TER	51 ± 13 Ω*cm^2	45 ± 15.8 Ω*cm^2	28.9 ± 3.7 Ω*cm^2	44 ± 6.8 Ω*cm^2

Table 4. Transepithelial Resistance (TER) Values for all Cell Lines. The TER is lower in the Ser471A cell line compared to that of the others. Data expressed as Mean ± SD.

Permeability:

The permeability for the sodium, chloride, and potassium ions were calculated as well. When the MDCK monolayer was challenged with an apical-to-basal chemical gradient (135 mM NaCl at the apical side to 33.75 mM NaCl at the basal side), it was found that a positive diffusional potential (Figure 15) had developed across the monolayer (with the basal side as zero reference). This positive diffusional potential was consistent when the MDCK monolayer was challenged with an apical-to-basal chemical gradient using potassium ions instead. The trend was seen for all the MDCK cell lines without any significant differences among the groups. The experiment was also performed with a basal-to-apical chemical gradient and found that the direction of gradient had no effects on the measurements of diffusional potential. The Goldman-Hodgkin-Katz equation calculated the ratio of permeability of sodium over chloride at 1.62 ± 0.3 for the wild type cells compared to 1.35 ± 0.07 in cells expressing the Ser471A transgene ($P < 0.05$). (Table 5, Figure 11). This suggests that either the P_{Na} was lower or P_{Cl} was higher in this cell line. The equation was also used to calculate the ratio of permeability of potassium over chloride at 1.17 ± 0.06 for Ser471A cell line and 1.35 ± 0.11 for the wild type ($P < 0.05$) (Table 5). After calculating the absolute permeability of the ions using the Kimizuka-Koketsu equation, it was found that the permeability for sodium, chloride, and potassium were significantly higher in the Ser471A MDCK cells compared to that of the WTOcc, Ser471D, and parental ($P < 0.05$, $n = 12$) (Table 5). There was a 28% increase in P_{Na}, an increase of 24% in P_k, and an approximate 54% increase in the P_{Cl} in the Ser471A line compared to WTOcc. Therefore, the decreased permeability ratio for both sodium over chloride and potassium over chloride in the Ser471A cell line can be attributed to the overall net increase in P_{Cl}.

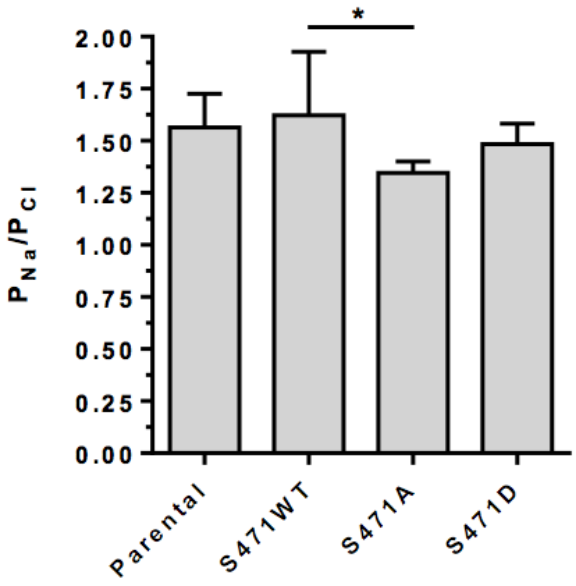

Figure 11. Permeability Ratio for Sodium over Chloride. Data expressed as Mean ± SD (n = 12). *P < 0.05 compared to parental, WTOcc, and Ser471D.

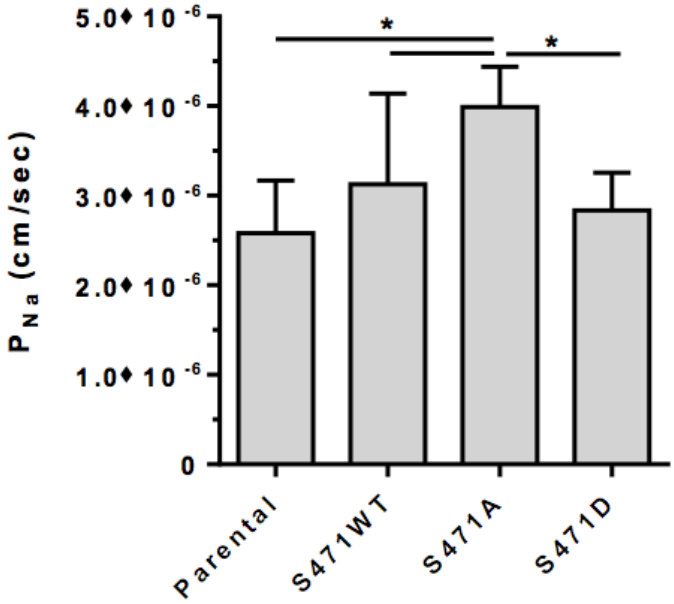

Figure 12. Absolute Permeability of Sodium for Each Cell Line (n=12). Data expressed as Mean ± SD (n = 12). *P < 0.05 compared to parental, WTOcc, and Ser471D.

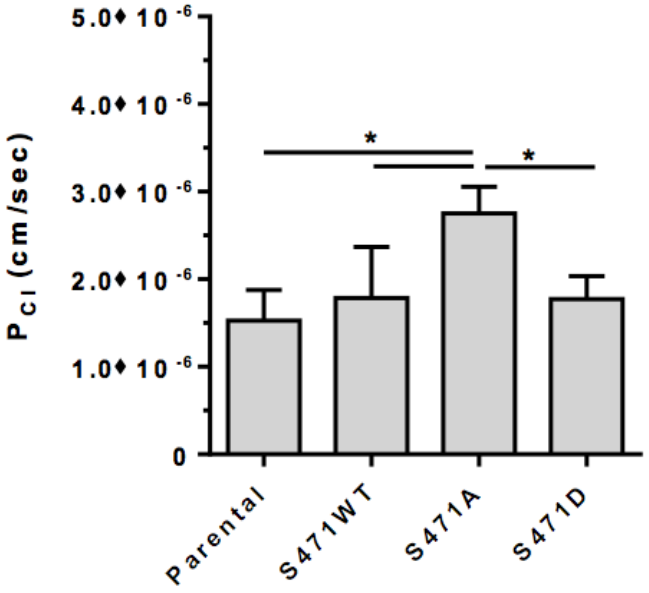

Figure 13. Absolute Permeability of Chloride for Each Cell Line (n=12). Data expressed as Mean ± SD (n = 12). *P < 0.05 compared to parental, WTOcc, and Ser471D.

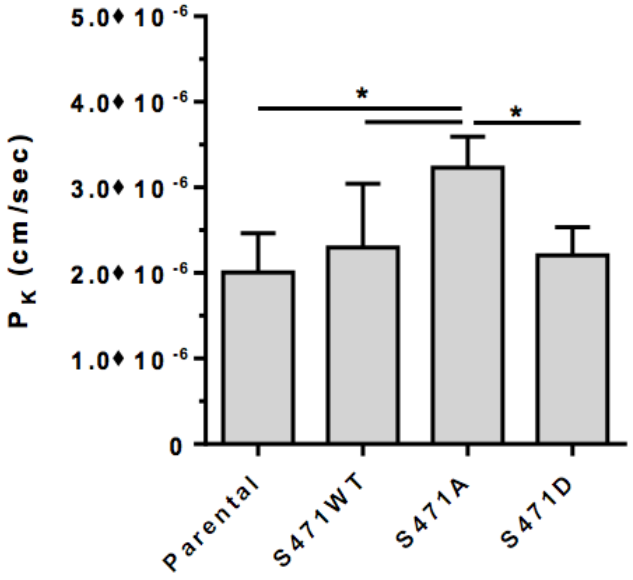

Figure 14. Absolute Permeability of Potassium for Each Cell Line (n=12). Data expressed as Mean ± SD (n = 12). *P < 0.05 compared to parental, Ser471WT, and Ser471D.

Group	Parental	Ser471WT	Ser471A	Ser471D
P_{Na}/P_{Cl}	1.56 ± 0.16	1.62 ± 0.3	1.35 ± 0.07	1.48 ± 0.09
P_K/P_{Cl}	1.31 ± 0.08	1.29 ± 0.12	1.18 ± 0.06	1.25 ± 0.06
P_{Na} (10^{-6} cm/s)	2.58 ± 0.58	3.13 ± 1	3.99 ± 0.45	2.84 ± 0.42
P_{Cl} (10^{-6} cm/s)	1.53 ± 0.35	1.79 ± 0.58	2.75 ± 0.31	1.77 ± 0.26
P_K (10^{-6} cm/s)	2.01 ± 0.46	2.30 ± 0.75	3.23 ± 0.36	2.21 ± 0.33

Table 5. Permeability Ratio and Absolute Permeability Data, (n= 12). Data expressed as Mean ± SD, n = 12.

Discussion:

Occludin is a hyperphosphorylated protein with a high degree of regulation in diverse cellular functions including barrier formation and regulation, cell migration, and division. Ser471 phosphorylation has been shown to enhance interaction with ZO-1 (Tash et al., 2012) but the cellular consequence of this phosphorylation site was unknown. This study has shown that introducing a phosphoinhibitory mutation, Ser471A, caused tight junction formation to be compromised. Concurrent work done in our lab revealed through immunocytochemistry imaging that the Ser471A cell line had breaks in the tight junction (Figure 5). In addition, ECIS studies revealed that the transepithelial resistance of the MDCK cells significantly decreased when transfected with Ser471A (Figures 6 and 7). Therefore, it was hypothesized that the Ser471A MDCK cell line would have non-selective ion flux because of the incomplete tight junction formation and lowered transepithelial resistance.

The quantitative results obtained using the Ussing chamber were consistent with the transepithelial resistance work done using the ECIS. In either set-up, the transepithelial resistance was significantly lower for the Ser471A cell line compared to the other three cell lines (i.e. parental, WTOcc, and Ser471D). This suggests that phosphorylation status of Ser471 plays an important role in determining tight junction integrity through perhaps interacting with ZO-1 to form a stable protein complex. By forming tighter junctions, occludin phosphorylated at Ser471 allows for greater transepithelial resistance and lower permeability for ions. When comparing the Ussing chamber values with those of other electrophysiological studies utilizing the apparatus, it was observed that the transepithelial resistance for MDCK with occludin (Yu et al., 2005) was similar to the transepithelial resistance of WTOcc MDCK cell line used in our study. In order to

test, however, if the change in transepithelial resistance was due to a specific flux of ions, the Goldman-Hodgkin-Katz and Kimizuka-Koketsu equations were utilized.

Using the Goldman-Hodgkin-Katz equation, the permeability ratio for sodium over chloride was always greater than one, regardless of the cell line, suggesting that there is an overall greater permeability to sodium ions compared to chloride ions, which is consistent with previous studies (Yu et al., 2005; Yu et al, 2009; Figure 15). After calculating the absolute permeabilities for the sodium, potassium, and chloride ions using the Kimizuka-Koketsu equation, there was a significant increase in permeability for all ions in the Ser471A cell line suggesting nonspecific ion flux. On the contrary, by placing a phosphomimetic mutation (i.e. Ser471D), we saw that the absolute permeability for all ions were similar to that of the WTOcc cell line. This strengthens the claim that phosphorylated Ser471 is involved in maintaining the integrity of the tight junction and strengthening the barrier to ion flux.

In addition, there was a decrease in the permeability ratio in the Ser471A cell line suggesting that there is a net increase in anion permeability compared to that of WTOcc. It has been shown that MDCK cells are cation selective with a relative permeability ratio, P_{Na}/P_{Cl}, of 1.7 (Misfeldt et al., 1976). This suggests that the absence of a phosphorylation site on Ser471A deregulates tight junction formation (i.e. disrupts tight junction integrity) allowing bigger anions, such as chloride, to cross the epithelium relatively easier. This effect may also be due to a steep charge gradient established by increasing the diffusion of the cations through gaps in the tight junction of the Ser471A cell line and therefore increasing the net positive charge on the apical side compared to the basal side. This increase in positive charge may be attracting more chloride ions (i.e. negative charge), which can now freely diffuse as well through the membrane due to poor tight junction formation in the Ser471A cell line, to the apical side resulting in the increased

permeability of the anion. This electrophysiological phenomenon was observed regardless of which side the charge gradient was set up (i.e. apical or basal). The permeability ratio for potassium over chloride ions followed the same trend as that described above for the sodium over chloride ions.

Previous studies of tight junctions have established a close association between the scaffolding protein, ZO-1, and the transmembrane protein, occludin, and identified multiple phosphorylation sites as potential regulators of their interaction. It has also been shown in vivo that the occludin:ZO-1 interaction is modulated by phosphorylation events on specific sites (Balda et al., 1996; Elias et al., 2009; Kale et al., 2009; Raleigh et al., 2011; Rao et al., 2002). In occludin, four of these sites segregate structurally and possibly functionally – two adjacent to the primary interaction site (Ser471 and Y474) in the acidic head and two in the secondary interface (Ser490 and Ser508) on the basic face (Tash et al., 2012). Y474 phosphorylation is associated with binding p85 of phosphatidylinositol 3-kinase at the leading edge of migrating cells (Du et al., 2010) while Ser490 and Ser508 are associated with vascular permeability after VEGF treatment (Sundstrom et al., 2009) or HIV encephalitis (Yamamoto et al., 2008). Ser471, however, may have a role in in regulating ZO-1 binding. The CC peptide 468-475, containing Ser471, was shown to be more effective at blocking PSG and ZO-1 capture when phosphorylated at Ser471 (pSer471) (Tash et al., 2012). This suggests, along with data acquired in our study, that phosphorylation of occludin at Ser471 may regulate proper tight junction formation in vivo and as a result form more stable tight junctions.

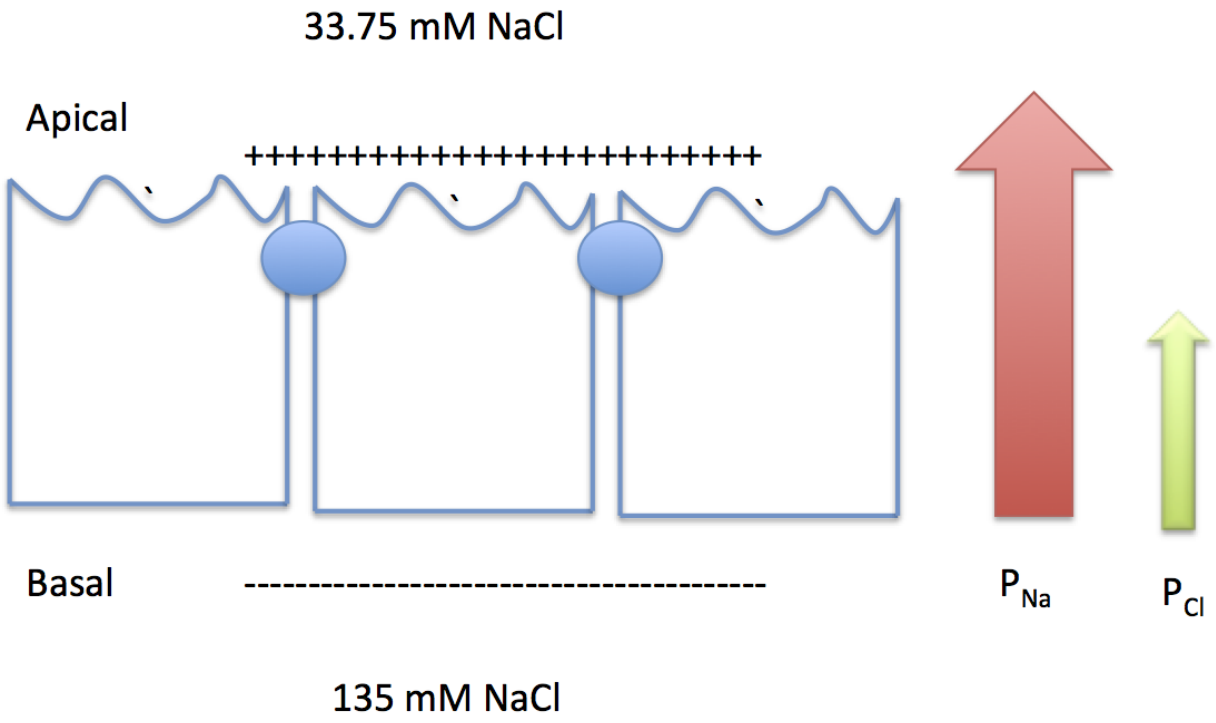

Figure 15. Diagram illustrating Ionic Flux in Response to an Ussing Chamber Dilution. The positive dilution potential recorded when the apical side was being filled with 0.25[Na+]HR solution. The sodium ions responded to the newly formed gradient by freely diffusing to the apical side making the net charge on this side of the membrane more positive compared to the basal side (the reference side).

Concurrent Research:

Ongoing research by Mark Bolinger as part of his dissertation reveals that Ser471 of occludin may contribute to cell packing and assembly of the tight junctions. Cell lines expressing Ser471A proliferate normally but have reduced packing and tight junction formation. Cells normally stop proliferation through contact inhibition involving signaling from adherens junctions through the Hippo pathway (Figure 16).

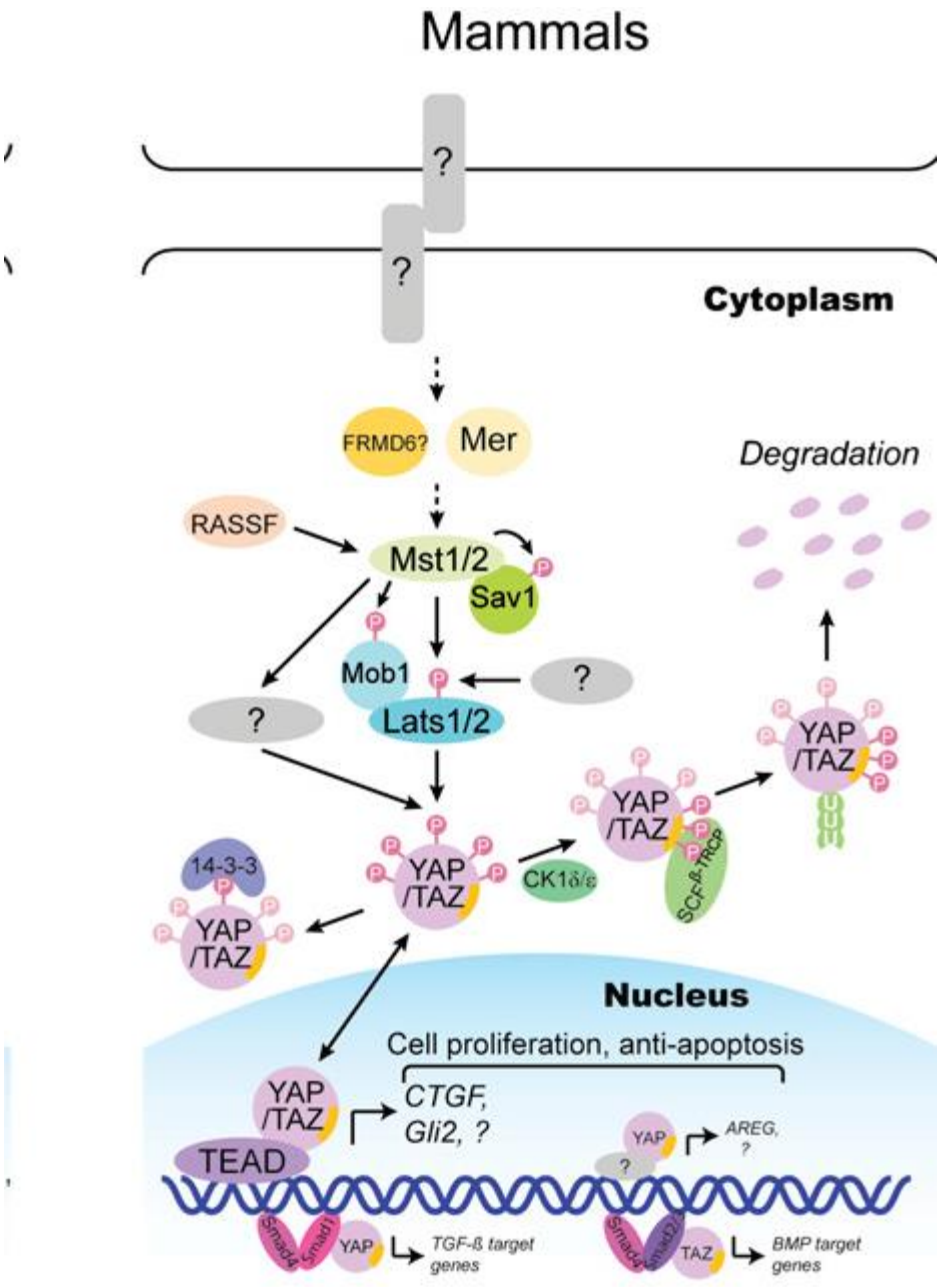

Figure 16. Model of the Hippo Pathway in Mammals. After initial cell to cell contact, there is an intracellular cascade that triggers the phosphorylation of YAP/TAZ priming it for either inhibition or degradation. This allows for TEAD to transcribe mRNA responsible for cell proliferation and anti-apoptosis leading to the hypertrophic phase (Zhao et al., 2010).

When two cells come in contact with one another through various interactions, they form a stable connection. An example of this interaction is when two E-cadherin proteins on adjacent cells form a bond and bring two cells in contact with one another. The current research reveals that in MDCK epithelial monolayers, after this initial interaction, the cells experience a period of packing in which the cells proliferate without hypertrophic growth yielding smaller cells at high density followed by tight junction formation yielding densely packed and highly regular cells with tight junctions on all sides (Figure 17). Research by Mark Bolinger revealed that Ser471A cells fail to pack and form tight junctions; this was consistent with the immunocytochemistry imaging done earlier that revealed breaks in the tight junction for Ser471A cell lines (Figure 5). An identical phenotype could be achieved with inhibition of cell cycle progression using roscovitin treatment after cell monolayers forms but before packing. Further, GRK4, 5, or 6 was identified as a kinase for Occ Ser471 and inhibitors of this kinase could also replicate the phenotype preventing or delaying packing and tight junction formation. These data suggest that phosphorylation of occludin Ser471 does contribute to regulating tight junction formation and likely accounts for the nonspecific ion flux through the gaps in the tight junctions of the transgenic Ser471A MDCK cells. However, the effect of Ser471 phosphorylation appears much broader than directly affecting tight junction formation and contributes to control of cell packing and subsequent tight junction formation.

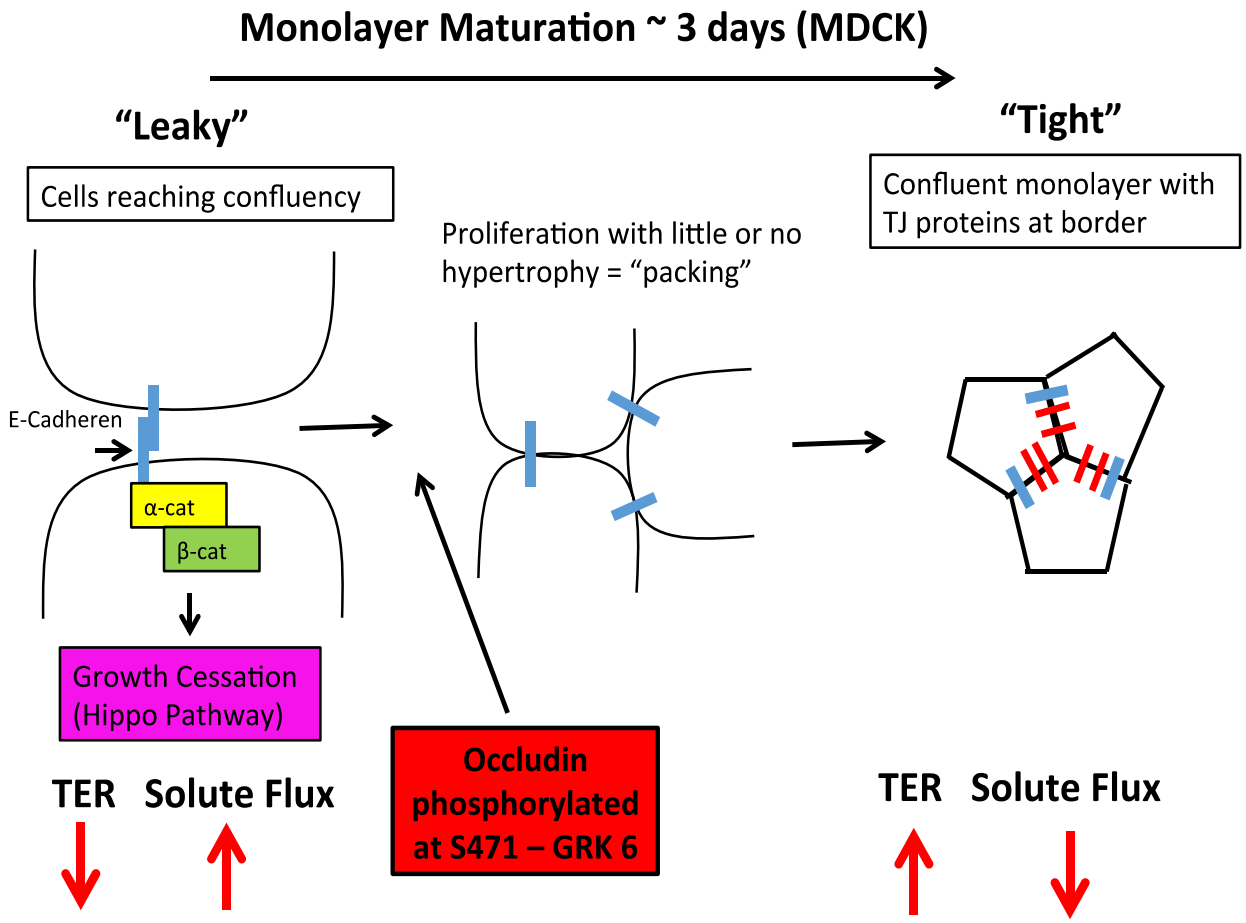

Figure 17. Diagram Detailing the Formation of Tight Junctions. It has been shown that the timely cell packing contributes to tight junction formation. Ser471A causes the barrier to not form properly by preventing cell packing and directly impacting tight junction formation (image courtesy of Mark Bolinger).

Limitations:

One drawback of the study was that we did not account for liquid junction potential across agar bridge pipettes. The junction between the agar in the bridges and the apical or basolateral solution represents a static liquid junction. To account for this error, a 3M KCl was used in the bridges because this minimizes the liquid junction potential. Furthermore, in symmetrical solutions, the liquid junction potential of the apical and basolateral pipettes should cancel each other out. However, when asymmetrical solutions are used to measure diffusion potentials, which is the principal method used to determine relative permeability of ions, the liquid junction potential of the two pipettes differ and a significant error can be introduced.

There are two major problems while attempting to predict the liquid junction potentials of 3M KCl pipettes (Barry and Diamond, 1970). First, prolonged immersion of the 3M KCl pipettes in the bathing solution introduces the bathing solution (i.e. ringer solution) into the pipette tip, changing its composition so that the apparent liquid junction potential become dependent on the history of the pipette. Second, even with fresh 3M KCl, the empirically determined liquid junction potential differs from the theoretical value and is somewhat unpredictable (Yu et al., 2009).

In our setup, we tried correcting for this error by using a blank insert, a common approach used by many other investigators in this field. In order to calculate the proper transepithelial potential using this method, we would first measure the potential across the blank insert, V_{EF}, and then subtract that value from the measured potential in the presence of the membrane, V_{EM}, to arrive at the true transmonolayer potential, V_M.

$$V_M = V_{EM} - V_{EF}$$

Where VEF = $V_L^b - V_L^a$ (i.e. the difference in liquid junction potential between the two pipettes).

However, this experimental design is flawed. The above formula assumes that there is no potential across the blank filter. In fact, it has been observed that the blank filter has 0.4 µm pores and is most likely freely permeable to small ions so it must behave as a liquid junction potential. Therefore, the correct relationship between the measured potential and the pipette potentials is the following equation (Yu et al., 2009):

$$VEF = (V_L^b - V_L^a) + V_F$$

where V_F is the voltage of the filter, which is typically ignored in most studies.

In order to correct for this liquid junction potential in the future, we will use the generalized Henderson-Planck equation (Barry and Diamond, 1970):

$$V_A - V_B = (RT/F)\, S_f \ln\{(\sum z_i^2 u_i a_i^B)/ (\sum z_i^2 u_i a_i^A)\}$$

$$S_f = [\sum(z_i u_i)(a_i^A - a_i^B)] / [\sum(z_i^2 u_i)(a_i^A - a_i^B)]$$

where z_i represents the charge of the ion, a_i is the activity of the ion on either the apical (A) or basal (B) side, and u_i is the mobility coefficient.

Name	z	u
Cl	-1	1.0388
K	1	1
Na	1	0.682
HEPES	-1	0.3
Ca	2	0.4048
Mg	2	0.361

Table 6. Charge and mobility values used to calculate the liquid junction potential for each ion in the HR solution (values courtesy of Dr. Bret Hughes).

Another drawback of the study was the use of only two cations (i.e. sodium and potassium) and one anion (i.e. chloride). In order to further validate the non-selectivity of the Ser471A cell line, more cations and anions need to be tested using the same protocol described above (i.e. diluting the Hepes ringer solution and utilizing the Ussing Chamber, the Goldman-Hodgkin-Katz, and Kimizuka-Koketsu equations to determine absolute ion permeability values) with various other cations (i.e. calcium, magnesium, etc.).

Acknowledgments:

I would like to thank my mentor, Dr. David Antonetti from Kellogg Eye Center, for giving me the opportunity to conduct an independent project and for his excellent guidance, patience, encouragement, and providing me with an excellent atmosphere for conducting research. I would also like to thank him for providing articles, images, and ideas referenced in this paper as well as for editing the thesis.

In addition, I would like to thank Mark Bolinger for platting cells and for also providing guidance in every step of the thesis process. He was always willing to help and give his best suggestions. Without his help and encouragement I would not have been able to successfully complete this research project.

I would also like to thank Dr. Bret Hughes from the Kellogg Eye Center for allowing me to use the Ussing chamber in his lab, providing his input to the project, and guidance regarding the electrophysiology experiments performed.

References:

Alberts B, Johnson A, Lewis J, Raff M, Roberts K, Walter P. 2008. Molecular biology of the cell. 5th ed. New York (NY): Garland Science, Taylor & Francis Group, LLC. Chapter 19, Cell junctions, cell adhesion, and the extracellular matrix; p. 1131 – 1164.

Antonetti DA, Barber AJ, Hollinger LA, Wolpert EB, Gardner TW. 1999. Vascular endothelial growth factor induces rapid phosphorylation of tight junction proteins occludin and zonula occluden 1. A potential mechanism for vascular permeability in diabetic retinopathy and tumors. J. Biol. Chem. 274 (33), 23463-7.

Balda MS, Anderson JM, Matter K. 1996. The SH3 domain of the tight junction protein ZO-1 binds to a erine protein kinase that phosphorylates a region C-terminal to this domain. FEBS Lett. 399:326-332.

Berx G, Becker K-F, Hofler H, van Roy F. 1998. Mutation Update: Mutations of the human E-cadherin (CDH1) gene. Hum Mutat 12:226-237.

Cereijido M, Robbins ES, Dolan WJ, Rotunno CA, and Sabatini DD. 1978. Polarized monolayers formed by epithelial cells on a permeable and translucent support. J. Cell Biol. 77:853-880.

Chan LS. 2011. Bullous pemphigoid. eMedicine.

Claude P, Goodenough DA. 1973. Fracture faces of zonulae occludentes from “tight” and “leaky” epithelia. J. Cell Biol. 58:390-400.

Elias BC, Suzuki T, Seth A, Giorgianni F, Kale G, Shen L, Turner JR, Naren A, Desiderio DM, Rao R. 2009. Phosphorylation of Tyr-398 and Tyr 402 in occludin prevents its interaction with ZO-1 and destabilizes its assembly at the tight junctions. J. Biol. Chem. 284:1559-1569.

Fanning AS, Jameson BJ, Jesaitis LA, Anderson JM. 1998. The tight junction protein ZO-1 establishes a link between the transmembrane protein occludin and the actin cytoskeleton. J. Biol. Chem. 273:29745-29753.

Farquhar MG, Palade GE. 1963. Junctional complexes in various epithelia. J. Cell Biol. 17:375-412.

Furuse M, Hirase T, Itoh M, Nagafuchi A, Yonemura S, Tsukita S. 1993. Occludin: a novel integral membrane protein localizing at tight junctions. J. Cell Biol. 123, 1777-1788.

Furuse M, Fujita K, Hiiragi T, Fujimoto K, Tsukita S. 1998. Claudin-1 and -2: novel integral membrane proteins localizing at tight junctions with no sequence similarity to occludin. J. Cell Biol. 141, 1539-1550.

Harhaj NS, Felinski EA, Wolpert EB, Sundstrom JM, Gardner TW, Antonetti DA. 2006. VEGF activation of protein kinase C stimulates occludin phosphorylation and contributes to endothelial permeability. Invest. Opthalmol. Visual Sci. 47 (11), 5106-15.

Kale G, Naren AP, Sheth P, Rao RK. 2003. Tyrosine phosphorylation of occludin prevents its interaction with ZO-1, ZO-2, and ZO-3. Biochem Biophys Res Commun. 302:324-329.

Lai-Cheong JE, Liu L, Sethuraman G, Kumar R, Sharma VK, Reddy SR et al. 2007. Five new homozygous mutations in the KIND1 gene in Kindler syndrome. J Invest Dermatol 127:2268-2270.

Li Bi W, Parysek LM, Wamick R, Stambrook PJ. 1993. In vitro evidence that metabolic cooperation is responsible for the bystander effect observed with HSV tik retroviral gene therapy. Hum. Gene Ther. 4:725-731.

Li H, Sheppard DN, Hug MJ. 2004. Transepithelial electrical measurements with the Ussing chamber. J. of Cystic Fibrosis. 3:123-126.

Misfeldt DS, Hamamoto ST, Pitelka DR. 1975. Transepithelial transport in cell culture. Proc. Nat. Acad. Sci. USA. 73:1212-1216.

Murakami T, Felinski EA, Antonetti DA. 2009. Occludin phosphorylation and ubiquitination regulate tight junction trafficking and vascular endothelial growth factor-induced permeability. J. Biol. Chem. 284:21036-21046.

Raleigh DR, Marchiando AM, Zhang Y, Shen L, Sasaki H, Wang Y, Long M, Turner JR. 2010. Tight junction-associated MARVEL proteins marveld3, tricellulin, and occludin have distinct but overlapping functions. Mol. Biol. Cell. 21:1200-1213.

Raleigh DR, et al. 2011. Occludin S408 phosphorylation regulates tight junction protein interactions and barrier function. J. Cell Biol. 193:565-582.

Rao RK, Basuroy S, Rao VU, Karnaky KJ, Jr, Gupta A. 2002. Tyrosine phosphorylation and dissociation of occludin-ZO-1 and E-cadherin-beta-catenin complexes from the cytoskeleton by oxidative stress. Biochem. J. 388:471-481.

Saitou M, Furuse M, Sasaki H, Schulzke JD, Fromm M, Takano H, Noda T, Tsukita S. 2000. Complex phenotype of mice lacking occludin, a component of tight junction strands. Mol. Biol. Cell. 11:4131-4142.

Schneeberger EE, Lynch RD. 2004. The tight junction: a multifunctional complex. Am. J. Physiol. Cell Physiol. 286, C1213-C1228.

Shen L, Weber CR, Turner JR. 2008. The tight junction protein complex undergoes rapid and continuous molecular remodeling at steady state. J. Cell Biol. 181:683-695.

Staehelin LA, 1974. Structure and function of intercellular junctions. Int. Rev. Cytol. 39, 191-283.

Stevenson BR, Siliciano JD, Mooseker MS, Goodenough DA. 1986. Identification of ZO-1: a high molecular weight polypeptide associated with the tight junction (Zonula Occludens) in a variety of epithelia. J. Cell Biol. 103:755-766.

Sundstrom JM, Tash BR, Murakami T, Flanagan JM, Bewley MC, Stanley BA, Gonsar KB, Antonetti DA. 2009. Identification and analysis of occludin phosphosites: a combined mass spectrometry and bioinformatics approach. J. Proteome Res. 8:808-817.

Suzuki T, Elias BC, Seth A, Shen L, Turner JR, Giorgianni F, Desiderio D, Guntaka R, Rao R. 2009. PKC eta regulates occludin phosphorylation and epithelial tight junction integrity. Proc. Natl. Acad. Sci. USA. 106:61-66.

Tash BR, Bewley MC, Russo M, Keil JM, Griffin KA, Sundstrom JM, Antonetti DA, Tian F, Flanagan JM. 2012. The occludin and ZO-1 complex, defined by small angle X-ray scattering and NMR, has implications for modulating tight junction permeability. Proc. Natl. Acad. Sci. USA. 109:10855-10860.

Umeda K, Ikenouchi J, Katahira-Tayama S, Fursue K, Sasaki H, Nakyama M, Matsui T, Tsukita S, Furuse M. 2006. ZO-1 and ZO-2 independently determine where claudins are polymerized in tight junction strand formation.

Wolff K, Goldsmith L, Gilchrest B, Katz S, Paller A, Leffell D. 2007. Fitzpatrick's Dermatology in General Medicine. 7th ed. New York (NY): Mcgraw-Hill. Chapter 54. Bullous Pemphigoid.

Woods DF, Bryant PJ. 1993. Apical junctions and cell signaling in epithelia. J. Cell Sci. 17:171-181.

Yamamoto M, et al. 2008. Phosphorylation of claudin-5 and occludin by rho kinase in brain endothelial cells. Am. J. Pathol. 172:521-533.

Yu AS, McCarthy KM, Francis SA, McCormack JM, Lai J, Rogers RA, Lynch RD, Schneeberger EE. 2005. Knockdown of occludin expression leads to diverse phenotypic alterations in epithelial cells. Am. J. Physiol.: Cell Physiol. 288 (6), C1231-41.

Yu AS, Cheng MH, Angelow S, Gunzel D, Kanzawa SA, Schneeberger EE, Fromm M, Coalson RD. 2009. Molecular basis for cation selectivity in claudin-2-based paracellular pores: identification of an electrostatic interaction site. J. Gen. Physiol. 133:111-127.

Zhao B, Li L, Lei Q, and Guan K-L. 2010. The Hippo-YAP pathway in organ size control and tumorigenesis: an updated version. Genes & Dev. 24:862-874.

Zhu J, Shang, Y, Xia C, Wang W, Wen W, and Zhang M. 2011. Guanylate kinase domains of the MAGUK family scaffold proteins as specific phosphor-protein-binding modules. The EMBO Journal. 30:4986-4997.